Experimental Evidence for Magnetorotational Instability in a Taylor-Couette Flow under the Influence of a Helical Magnetic Field

Frank Stefani, Thomas Gundrum, and Gunter Gerbeth

Forschungszentrum Rossendorf, P.O. Box 510119, D-01314 Dresden, Germany

Günther Rüdiger, Manfred Schultz, and Jacek Szklarski

Astrophysikalisches Institut Potsdam, An der Sternwarte 16, D-14482 Potsdam, Germany

Rainer Hollerbach

Department of Applied Mathematics, University of Leeds, Leeds, LS2 9JT, United Kingdom
(Received 20 June 2006; published 1 November 2006)

A recent Letter [R. Hollerbach and G. Rüdiger, Phys. Rev. Lett. **95**, 124501 (2005)] has shown that the threshold for the onset of the magnetorotational instability in a Taylor-Couette flow is dramatically reduced if both axial and azimuthal magnetic fields are imposed. In agreement with this prediction, we present results of a Taylor-Couette experiment with the liquid metal alloy GaInSn, showing evidence for the existence of the magnetorotational instability at Reynolds numbers of order 1000 and Hartmann numbers of order 10.

The role of magnetic fields in the cosmos is twofold: First, planetary, stellar, and galactic fields are a product of the homogeneous dynamo effect in electrically conducting fluids. Second, magnetic fields are also believed to play an active role in the formation of stars and black holes, by enabling outward transport of angular momentum in accretion disks via the magnetorotational instability (MRI) [1]. Considerable theoretical and computational progress has been made in understanding both processes. The dynamo effect has even been verified experimentally, in large-scale liquid sodium facilities in Riga and Karlsruhe, and continues to be studied in laboratories around the world [2]. In contrast, obtaining the MRI experimentally has been less successful thus far [3]. Actually, an MRI-like instability has been observed on the background of a turbulent spherical Couette flow [4], but the original idea that MRI would destabilize an otherwise stable flow was not realized in experiment up to present.

If only an axial magnetic field is externally applied, the azimuthal field that is necessary for the occurrence of the MRI must be produced by induction effects, which are proportional to the magnetic Reynolds number (Rm) of the flow. But why not substitute this induction process simply by externally applying an azimuthal magnetic field as well? This question was at the heart of the Letter [5], where it was shown that the MRI is then possible with far smaller Reynolds (Re) and Hartmann (Ha) numbers. In this Letter, we report experimental verification of this idea, presenting evidence of the MRI in a liquid metal corotating Taylor-Couette (TC) cell with externally imposed axial and azimuthal (i.e., helical) magnetic fields.

The heart of our facility "PROMISE" (Potsdam Rossendorf Magnetic Instability Experiment) is a cylindrical vessel *V* made of copper (see Fig. 1). The use of copper

was motivated by the fact that the instability usually occurs at lower Reynolds and Hartmann numbers for the case of ideally conducting boundaries than for nonconducting boundaries [6]. The inner wall is 10 mm thick and extends in radius from 22 to 32 mm; the outer wall is 15 mm thick,
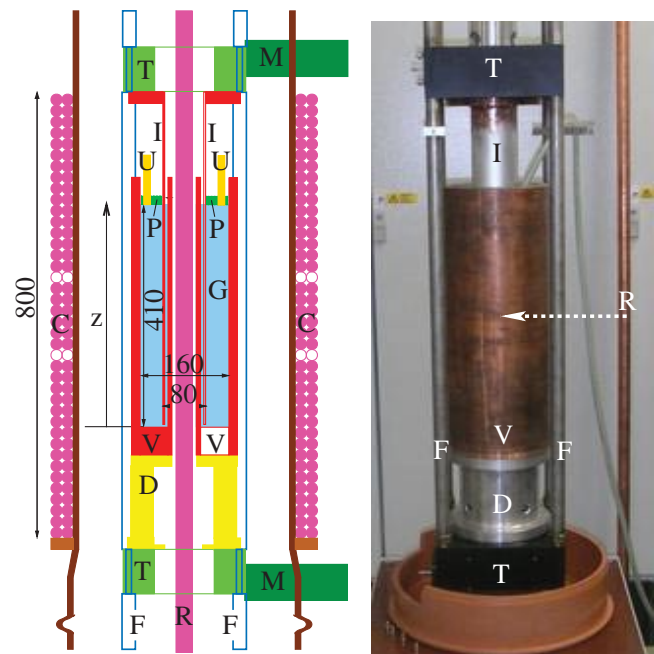

FIG. 1 (color).   Sketch (left) and photograph (right) of the central module of the PROMISE facility. *V*—copper vessel, *I*—inner cylinder, *G*—GaInSn, *U*—two ultrasonic transducers, *P*—Plexiglas lid, *T*—high precision turntables, *M*—motors, *F*—frame, *C*—coil, *R*—central rod. The dimensions are in millimeters. When the experiment is running, the rod *R* in the right picture goes through the center of the cylinders.

extending from 80 to 95 mm in r. This vessel is filled with the eutectic alloy $Ga^{67}In^{20.5}Sn^{12.5}$, which has the advantage of being liquid at room temperatures. The physical properties of GaInSn at 25 °C are density $\rho = 6.36 \times 10^3$ kg/m³, kinematic viscosity $\nu = 3.40 \times 10^{-7}$ m²/s, and electrical conductivity $\sigma = 3.27 \times 10^6$ $(\Omega\,\text{cm})^{-1}$. The magnetic Prandtl number is then $\text{Pm} = \mu_0\sigma\nu = 1.40 \times 10^{-6}$.

The copper vessel V is fixed, via an aluminum spacer D, on a precision turntable T; the outer wall of the vessel thus serves as the outer cylinder of the TC cell. The inner cylinder I of the TC flow is fixed to an upper turntable and is immersed into the GaInSn from above. It has a thickness of 4 mm, extending in radius from 36 to 40 mm. There is thus a gap of 4 mm between this immersed cylinder I and the inner wall of the containment vessel. The actual TC cell then extends in the radial direction over a cylindrical gap of width $d = r_{\text{out}} - r_{\text{in}} = 40$ mm from the outer surface of the inner cylinder at $r_{\text{in}} = 40$ mm to the inner surface of the outer wall of the containment vessel V at $r_{\text{out}} = 80$ mm and in the axial direction over the liquid metal height of 0 mm $\leq z \leq 410$ mm. At the moment, the upper end plate is a Plexiglas lid P fixed to the frame F. In contrast, the bottom is simply part of the copper vessel and, hence, rotates with the outer cylinder. There is thus a clear asymmetry in the end plates, with respect to both their rotation rates and electrical conductivities.

Note also that the tolerance of the key components of the apparatus is not quite at the $\sim 10^{-2}$ mm level that can be achieved in ordinary, hydrodynamic TC experiments, e.g., [7]. For example, in order to ensure a well-defined electrical contact between the GaInSn and the walls, it is necessary to intensively rub the fluid into the copper. Because of the resulting abrasion, the accuracy of the copper cylinders is certainly not better than 10^{-1} mm. The Reynolds number $\text{Re} = 2\pi f_{\text{in}} r_{\text{in}} d/\nu$ is $O(10^3)$, which is considerably greater than the critical value $\text{Re}_c = 68$ for the transition to vortical flow in the nonmagnetic TC problem for this radius ratio (with stationary outer cylinder).

Axial magnetic fields of order 10 mT are produced by a double-layer coil (C). The omission of windings at two symmetric positions close to the middle resulted from a coil optimization to maximize the homogeneity of the axial field throughout the volume occupied by the liquid. This coil is fed by a power supply that can deliver up to 200 A. The azimuthal field, also of order 10 mT, is generated by a current through a water-cooled copper rod R of radius 15 mm. The power supply for this axial current delivers up to 8000 A.

At present, the measuring instrumentation consists exclusively of two ultrasonic transducers with a working frequency of 4 MHz; these are fixed into the Plexiglas lid, 15 mm away from the outer copper wall, flush mounted at the interface to the GaInSn. Using ultrasound Doppler velocimetry (UDV) [8], they provide full profiles of the axial velocity ν_z along the beam lines parallel to the axis of rotation. The spatial resolution in axial direction is

0.685 mm; the time resolution is 1.84 sec. The width of the beam (over which ν_z is averaged) is approximately 8 mm, according to the diameter of the ultrasonic transducers. A similar measuring system for the axial velocity components in TC experiments was first described by Takeda *et al.* [9]. The comparison of the two signals from two opposite sensors is important in order to clearly distinguish between the expected axisymmetric ($m = 0$) MRI mode [6] and certain $m = 1$ modes which also play a role in some parameter regions of the experiment.

Typically, the duration of the experimental runs was 1900 s, after a waiting time of 1 h. Such a long waiting time was chosen not only due to the hydrodynamic gap diffusion time $\tau_{\text{gap}} = d^2/\nu$ but also due to our numerical predictions of rather small growth rates of the MRI mode in helical fields (see also [10]).

As a consequence of the reflection symmetry breaking under the influence of a helical magnetic field [11], the usual Taylor vortices of the TC flow (which we had clearly identified in preexperiments without magnetic field) are replaced by an oscillatory axisymmetric vortex flow that propagates in a unique direction along the vertical axis [5]. This direction depends on the screw sense of the magnetic field and the direction of the flow rotation (all results presented in this Letter are for an upward traveling wave). This traveling wave appears already at $\mu := f_{\text{out}}/f_{\text{in}} = 0$, although with a very low frequency. With increasing μ, the frequency increases and typically reaches a value of $0.2f_{\text{in}}$ at the Rayleigh value $\mu_{\text{Ray}} = (r_{\text{in}}/r_{\text{out}})^2 =: \eta^2$ (we have $\eta = 0.5$ here; hence, $\mu_{\text{Ray}} = 0.25$). The crucial point now is that, under the influence of helical magnetic fields, the critical Reynolds numbers remain relatively small increasingly far above the Rayleigh value, where nothing special happens. Typically, this shift to larger μ becomes larger for increasing values of the ratio $\beta := B_\varphi(r = r_{\text{in}})/B_z$ of azimuthal field to axial field.

Another typical feature of the MRI is that, for fixed Re, it sets in at a certain critical value of the Hartmann number $\text{Ha} = B_z(r_{\text{in}}d\sigma/\rho\nu)^{1/2}$ and disappears again at some higher value. In this Letter, we focus exclusively on experimental results which substantiate this behavior.

All results presented in the following are for rotation rates of $f_{\text{in}} = 0.06$ s⁻¹ and $f_{\text{out}} = 0.0162$ s⁻¹, i.e., for $\mu = 0.27$, above the Rayleigh value $\mu_{\text{Ray}} = 0.25$. Figure 2 documents a selection of seven experimental runs for coil currents I_{coil} between 0 and 120 A. In each case, the axial current I_{rod} was fixed to 6000 A. The color coding of the plots indicates the axial velocity component ν_z measured along the ultrasound beam, from which we have subtracted the z-dependent time average in order to filter out the two Ekman vortices which appear already without any magnetic field. These vortices, characterized by inward radial flows close to the upper and lower end plates, show up in our UDV data in the form of positive and negative axial velocities, separated approximately at mid-height by a rather sharp boundary. This boundary most
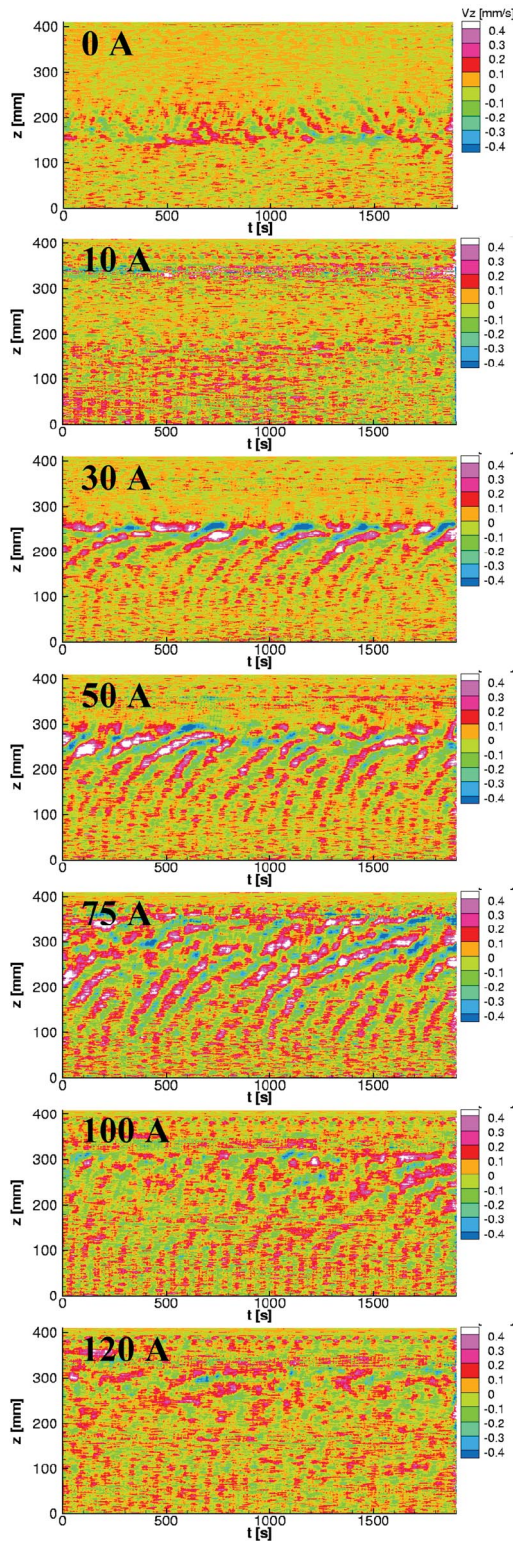
FIG. 2 (color). Measured axial velocities as functions of time and depth, for different coil currents.

middle part of the cylinder. One might speculate that, due to the (jetlike) radial outward flow there, fluid with lower angular momentum is transported outward, which leads to a locally steeper decrease of v_φ than what would be expected from the rotation ratio μ of outer to inner cylinder [12]. At $z \sim 270$ mm, i.e., close above the radial outflow region, the wave dies away.

For increasing I_{coil}, this traveling wave becomes more and more dominant, until at 75 A it fills essentially the entire cylinder. Some refraction of the wave remains visible in the radial outflow region approximately at midheight. Increasing I_{coil} even further, though, at 120 A this wave ceases to exist, and we again have a rather featureless flow. This is shown more quantitatively in Fig. 3, where we show the power spectral density (PSD) for the axial velocity for 5 selected values of I_{coil}. Actually, this PSD represents an average over the interval 102 mm $< z <$ 190 mm which has been chosen since it lies in front of the jetlike structure where the traveling MRI mode undergoes some refraction. A feature common to all five curves is the appearance of the rotation rates of the inner and outer cylinders. This reflects certain geometric imperfections of the facility, probably in the form of cylinder eccentricities or metal oxides sticking to some parts of the walls. There is also a certain peak approximately at the mean of the inner and outer cylinder frequencies, which, on closer inspection
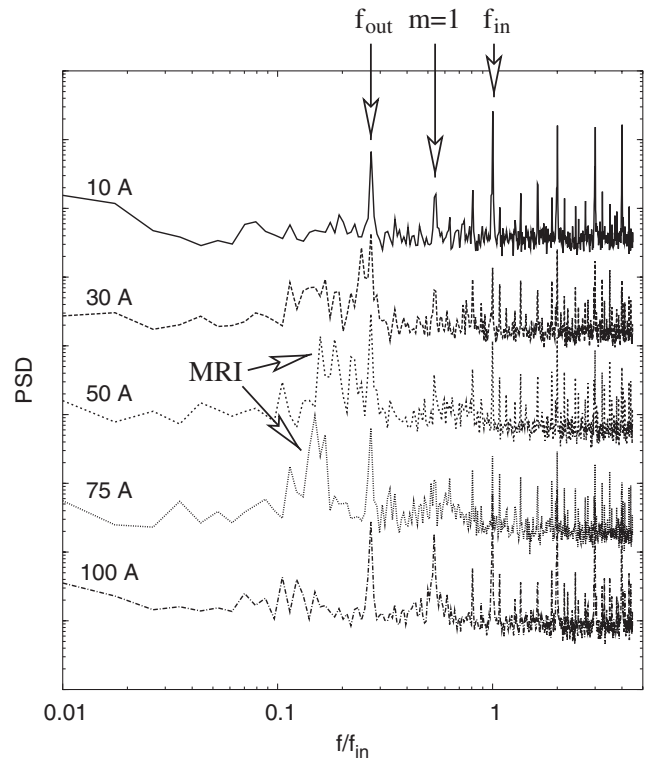

FIG. 3. Power spectra of the v_z fluctuations, averaged over 102 mm $< z <$ 190 mm, for 5 different coil currents. The frequencies of the inner and outer cylinders are indicated. The MRI is visible at 50 and 75 A. In addition to that, an $m = 1$ mode is also present.
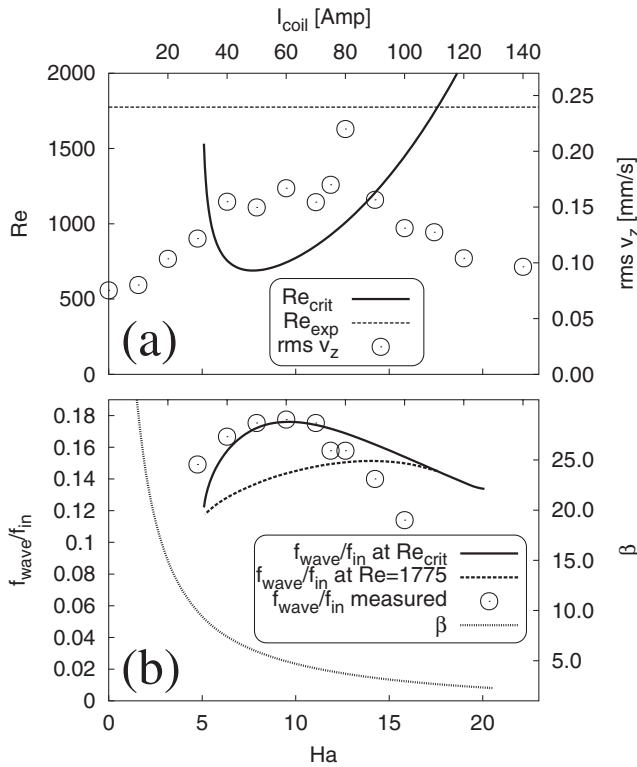
likely corresponds to a jetlike radial outflow in the center of the cylinder, as discussed in Ref. [12].

For $I_{coil} = 30$ A, we already observe a traveling wavelike structure which is, however, still restricted to the

FIG. 4. (a) Computed critical Reynolds numbers and measured rms of the axial velocity, for varying I_{coil} (and hence Hartmann numbers), for fixed $I_{rod} = 6000$ A. (b) Frequency f_{wave} of the traveling MRI wave, normalized to the rotation rate f_{in} of the inner cylinder. The ratio of azimuthal field to axial field β is also shown.

of the two transducer signals, turns out to be a nonaxisymmetric $m = 1$ mode. Most interesting for us here, however, is the MRI mode at $f/f_{in} \sim 0.1$–0.2. These frequencies have been analyzed in detail for all values of I_{coil} chosen in the experiment.

We now interpret these experimental data in the context of numerical predictions, obtained and cross-checked by various independent codes [5,13,14] for the solution of the linear eigenvalue problem in unbounded cylinders with ideally conducting radial boundaries. First, Fig. 4(a) shows the measured rms of v_z and the numerically computed critical Reynolds number, both in dependence on the Hartmann number. The higher values of rms of v_z in the interval 30 A $< I_{coil} < 110$ A (i.e., $4.7 < Ha < 17.4$) indicate the occurrence of MRI, which should also be expected since the experimental Reynolds number of 1775 is above the critical Reynolds number there.

Figure 4(b) compares the measured frequencies of the traveling wave, normalized to the rotation rate of the inner cylinder, with the frequencies computed for the infinite cylinder. The latter are actually given in two versions at Re_{crit} and at the experimental value Re $= 1775$. It is interesting that the difference between the two curves is relatively small. Hence, it might be anticipated that the normalized frequency in the nonlinear (saturated) regime

is probably also not far from these values. The measured frequencies are in reasonable correspondence with the computed ones and show a similar behavior, with a maximum close to Ha $= 10$.

In summary, we have provided experimental evidence for the existence of the MRI in current-free helical magnetic fields, by showing its appearance in a certain interval of Hartmann numbers, in qualitative agreement with numerical predictions. Further experimental results for other combinations of the governing parameters will be published elsewhere. Certainly, much numerical work remains to be done, including the treatment of the nonlinear regime, a more realistic handling of the magnetic radial boundary conditions, and a detailed investigation into the role of the magnetic axial boundary conditions. For later experiments, a symmetrization of the axial boundaries is envisioned. Connected with this, a suppression of the Ekman vortices by means of split rings (proposed in Ref. [12]; see also [15]) may also help to avoid special effects in the midheight of the cylinder.

[1] S. A. Balbus and J. F. Hawley, Astrophys. J. **376**, 214 (1991).
[2] A. Gailitis, O. Lielausis, E. Platacis, G. Gerbeth, and F. Stefani, Rev. Mod. Phys. **74**, 973 (2002).
[3] *MHD Couette Flows: Experiments and Models*, edited by R. Rosner, G. Rüdiger, and A. Bonanno, AIP Conf. Proc. No. 733 (AIP, New York, 2004).
[4] D. R. Sisan, N. Mujica, W. A. Tillotson, Y. M. Huang, W. Dorland, A. B. Hassam, T. M. Antonsen, and D. P. Lathrop, Phys. Rev. Lett. **93**, 114502 (2004).
[5] R. Hollerbach and G. Rüdiger, Phys. Rev. Lett. **95**, 124501 (2005).
[6] G. Rüdiger, R. Hollerbach, M. Schultz, and D. A. Shalybkov, Astron. Nachr. **326**, 409 (2005).
[7] F. Schultz-Grunow, Z. Angew. Math. Mech. **39**, 101 (1959).
[8] A. Cramer, C. Zhang, and S. Eckert, Flow Meas. Instrum. **15**, 145 (2004).
[9] Y. Takeda, W. E. Fischer, J. Sakakibara, and K. Ohmura, Phys. Rev. E **47**, 4130 (1993).
[10] W. Liu, J. Goodman, I. Herron, and H. Ji, astro-ph/0606125.
[11] E. Knobloch, Phys. Fluids **8**, 1446 (1996).
[12] A. Kageyama, H. Ji, J. Goodman, F. Chen, and E. Shoshan, J. Phys. Soc. Jpn. **73**, 2424 (2004).
[13] G. Rüdiger, M. Schultz, and D. Shalybkov, Phys. Rev. E **67**, 046312 (2003).
[14] F. Stefani and G. Gerbeth, in Ref. [3], p. 100.
[15] R. Hollerbach and A. Fournier, in Ref. [3], p. 114.